MICRITIC LIMESTONES OF THE MIDDLE EAST: INFLUENCE OF WETTABILITY, PORE NETWORK AND EXPERIMENTAL TECHNIQUE ON DRAINAGE CAPILLARY PRESSURE CURVE

Benjamin SALLIER (Université de Genève), Gérald HAMON (Total)

This paper was prepared for presentation at the International Symposium of the Society of Core Analysts held in Toronto, Canada, 21-25 August 2005

ABSTRACT

Primary drainage capillary pressure curves are often used to assess the distribution of initial water saturation versus elevation above the FWL in oil reservoirs. This paper focuses on 1) the comparison between oil/water centrifuge tests and mercury injection 2) the effect of wettability alterations due to drilling fluids and laboratory procedures on the oil/water drainage Pc curve 3) relationship between wettability and pore structure.

Outcrop low permeability microporous limestones, representative of three different sedimentary facies of the Shuaiba formation in the Middle East have been used for this study. Companion samples were used to assess the influence of the different treatments. Porosity, permeability, X-ray tomography, probe permeametry, and NMR T2 curves were used to ensure that companion samples were very similar.

For each facies, the following first drainage capillary pressure curves were compared:

- Oil/water at strongly water-wet conditions with refined oil
- Oil/water with reservoir oils
- Oil/water with reservoir oil after aging with reservoir oil and cleaning
- Oil/water with refined oil after flush with oil base mud filtrate and cleaning
- Mercury injection

For each treatment, wettability tests were also performed to measure the prevailing wettability during the drainage process.

The main results are:

- Large discrepancies are observed between water/oil and mercury injection Pc curves, particularly in microporous facies. Discrepancies are very significant over the full saturation range. Suggestions based on the very low pore sizes of these microporous rocks are proposed to scale these results to reservoir conditions.
- Severe oil-base mud invasion may result in dramatic overestimates of the initial water saturation from first drainage Pc, even after core cleaning.
- “Irreducible” water saturation is a poor criterion for rock-typing in carbonates.
- Wettability variations within a carbonate reservoir might also be attributed to the topological differences between facies.

- The efficiency of cleaning processes in carbonates is dependent on the interplay between the macroporosity and the microporosity, for the same reservoir oil and for the same suite of solvents.

INTRODUCTION

Several types of core measurements are used in conjunction with log interpretation to assess the vertical distribution of oil saturation in a virgin reservoir. The capillary pressure curves for primary drainage are measured with different techniques and different fluid pairs: Mercury injection (MICP) and water-oil centrifugation are among the most widely used methods. The present study aims at: (1) comparing these two different techniques, (2) investigating the effects of preliminary contact between porous media and either crude oil or oil-base mud filtrate, and (3) understanding cleaning efficiency on drainage Pc curves. This study focused on carbonate facies, which were selected based on their similarity to carbonates from Middle East reservoirs.

Few comparisons between Pcs using different fluid pairs have been published and opposite conclusions have been drawn. Purcell [1] observed a good reconciliation between porous plate method (water-air) and mercury injection Pc curves (considering mercury contact angle $\theta Hg_{vapor} = 0°$($\theta Hg_{liquid} = 180°$)). But the author actually measured a mean value equal to 40° (140°) for the mercury-vacuum system. Melrose [2] showed on Berea samples that Hg-vacuum system led to significantly lower wetting phase saturations in the high Pc range than in the water-gas system whatever the technique. Sabatier [3] and Hamon [4] confirmed that mercury injection yields lower values of wetting phase saturation than the oil/brine systems in the high Pc range and Greder [5] highlighted the fact that the discrepancy increases as the permeability of reservoir samples decreases. According to Sabatier [3] capillary pressures for a gas-liquid system cannot be transposed into a liquid-liquid system. Furthermore capillary pressures derived from mercury injection would be especially doubtful for high clay content porous media. Masalmeh [6] illustrated for carbonate samples that, at a given normalized capillary pressure, lower wetting phase saturation was achieved in the oil-water system than Hg-air system. Newsham [7] showed for tight sands, that MICP curves generate saturations consistently lower than the ones obtained by ultracentrifugation in water gas system but Wells [8] presented opposite conclusions. The effect of wettability on primary drainage has received little attention. Although Morrow [9, 10] concluded that for first drainage Pc curves, the impact of wettability could be neglected for contact angle value less than 50°, Richardson [11] stated that air-oil was preferred for centrifuge tests on Prudhoe Bay to ensure that “since oil will tend to wet an imperfectedly clean surface whereas water may not. If cores are properly cleaned to be water-wet, use of an air-water system on extracted cores will yield valid data”. Since the 70’s, it has been agreed that more than half of reservoirs cannot actually be considered as strongly water wet (SWW) (Treiber [12]; Anderson [13]). Furthermore, several sources of wettability alteration have been identified (coring fluids, trip out, oxydation, drying) leading to further shift towards very poor water wetness when cores are received in the laboratory. Very efficient cleaning would then be required to reproduce the strongly water-wet conditions that are supposed to prevail during the primary drainage of oil.

SAMPLES SELECTION

Selection of facies showing strong analogies with Middle East reservoirs:

Three main criteria were chosen for the selection of samples: 1) being representative of some Middle East reservoirs, 2) reproducible and well defined initial wettability condition, and 3) large number of samples with very close petrophysical properties. This last ensures reliable comparisons between samples subjected to different treatments and was satisfied by use of strongly water-wet outcrop samples. As illustrated by figure 1, four sedimentary facies were selected on southern France Urgonian Fm. outcrops. These actually represent strong chronological, faciological and diagenetical equivalences with Kharaib or Shuaiba Fm. from the Middle East. Chalky textures and abundant microporosity in the micritic matrix characterise those facies. Using, Dunham's textural classification [14], the first sample, R4, is classified as grainstone presenting both macroporous (with intergranular porosity estimated at 50% of the bulk porosity) and microporous fraction (intercrystalline porosity). Orgon and R5 samples are thin grainstones and pure microporous facies, microporosity being located between micrite crystals (located in peloides, foraminiferous shells, etc.) Finally, the R3 facies is composed of disconnected macro vugs (representing 9% of the bulk porosity) dispersed in micritic matric (microporous fraction). All facies consist of pure calcite.

Selection of similar samples:

A large number of samples have been taken for each facies. On each sample, X-Ray Tomography, porosity, permeability measurements (figure 2), NMR T2 relaxation, and local permeability by probe permeametry were performed. Samples were thus selected to find the largest set of homogeneous samples with identical properties for each facies. MICP has been also used to confirm the petrophysical similarity of the samples.

EXPERIMENTAL PROCEDURES

All experiments were conducted at ambient conditions (21°C, atmospheric pressure), except for the ageing phase. Image analyses were realized from thin section, SEM and X-Ray Microtomography acquired at the European Synchrotron Radiation Facility (Grenoble, France). Table 2 shows the sequence of forced displacements by centrifugation, spontaneous displacements, fluid change and eventually cleaning or ageing phases performed for each sedimentary facies.

MICP: Liquid phase of mercury (Hg_{vap}-Hg_{liq} fluid couple) is injected into an evacuated sample (1cm diameter), with incremental pressures (up to 4000 bars).

Ultracentrifugation: All measures are made on companion plugs (diameter: 38mm, length: 50mm). After being fully saturated with brine and weighed, plugs are loaded in a sample holder, filled with oil and centrifuged at increasing speeds. Rotation speed, running times are computed and fluid production is measured automatically by specific software using a stroboscope adjusted to the centrifuge speed and a camera. Raw data are corrected by the second Forbes solutions ($S_{\alpha\beta RC}$, [15]).

Cleaning: After sampling at the outcrop and coring, all plugs are soxhlet extracted with chloroform at 80°C. After each centrifugation cycle (see Table 2), core plugs were

mounted on individual cells and flushed sequentially with toluene then isopropanol. Samples were oven-dried for 24 hours before porosity and gas permeability measurements.

Ageing: Core plugs containing crude oils at irreducible water saturation (Swi) were submerged in the same oil and aged in sealed pressure cells for 15 days at 80°C.

Fluids used: Brine composition is presented in Table 1. Two kinds of crude oils from two distinct reservoirs (*Li* and *La*), a refined oil (*Ma52*®), and a oil base mud filtrate (*Mud*) were selected (viscosities, densities and interfacial tension with brines are listed in Table 1). Oils were centrifuged during 5 minutes at a rotating speed of 1000 rpm before being used in displacement tests

Wettability test: Three kinds of wettability tests have been conducted. Amott Harvey (I_{AH}) and USBM methods (I_{USBM}) (Anderson [16] Cuiec [17], [18]) have been used. When cycles were stopped at oil residual saturation (see Table 2), only the wettability index to water Iw are presented. In addition, spontaneous water imbibition rates provide another measure of wettability (Xie and Morrow [19]) and have been used in most cases.

Recovery curves are presented as a function of a dimensionless timescale as defined by (Zhou and Morrow [20]; Zhang, Morrow and Ma, [21]).

RESULTS AND DISCUSSIONS

Irreducible water saturation:

Results from primary drainage experiments using the centrifuge technique are shown in Figure 3 for the four carbonates facies (Ma_{52}®-brine fluid system). Figure 3 shows the excellent agreement between water-oil primary drainage curves measured on several samples belonging to the same facies. It confirms both the similarity of the different samples and the reproducibility of the tests. Although large differences exist between R3, R4, and Orgon in both the entry capillary pressure and along the transition zone, Pc curves almost overlap at irreducible saturation. The irreducible water saturation appears to be a poor criterion for rock typing in carbonates (as pointed out by Masalmeh [6]).

Large discrepancies between water-oil and mercury injection Pc curves:

Figure 4 shows the comparison between MICP and water-oil (Ma52®-brine) Pc curves on three Orgon samples. The MICP curves are almost superimposed, confirming again the similarity of the different samples and the reproducibility of the tests. Large discrepancies between MICP and water-oil (Ma52®-brine) Pc curves are observed over the full saturation range when scaled by interfacial tensions. At any given Pc, wetting phase saturation is always higher for oil-water than for Hg_v-Hg_l fluid system. In other words, the ratio $Pc_{w/o}\sigma_{Hg}/Pc_{Hg}\sigma_{w/o}$ is always greater than 1. This ratio is presented in Figure 5 as a function of Sw for all facies. The experimental ratios range from 1 to 2 even though the same fluids and techniques were used in all experiments. Such large differences in $Pc_{w/o}\sigma_{Hg}/Pc_{Hg}\sigma_{w/o}$ can hardly be ascribed to the conventional values of the contact angles: A mercury contact angle (vapour phase) (θHg_v=40°), and a water-oil contact angle ($\theta_{w/o}$=0°) would result in a ratio $Pc_{w/o}\sigma_{Hg}/Pc_{Hg}\sigma_{w/o}$ = 1.3. The ratios $Pc_{w/o}\sigma_{Hg}/Pc_{Hg}\sigma_{w/o}$ seem to be larger amongst microporous facies (R5 and Orgon) and

minimal when the macroporosity is a large fraction of the total porosity, as in R4 facies. Several possible experimental issues were investigated. Water/oil interfacial tension, brine compositions, pore volume, porosity and permeability were checked before and after the centrifuge tests for each facies, but no significant variation was found. Centrifuge interpretation methods were also questioned. Although the parameters N and B proposed by Forbes [15] are slightly greater than the critical values for our experimental set-up, it cannot lead to discrepancies larger than 5 s.u. as illustrated by Figure 6a and 6b. In these figures, errors in saturations using the Forbes $S_{\alpha\beta RC}$ method have been compiled from the SCA survey [22]. The effects of water/oil, and Hg contact angles as well as pore angularity have also been investigated. All initial wettability tests (Ma52®-brine) indicated strongly water-wet rocks (see figure 7) and water-oil contact angle should be low. Buckley reports a contact angle of 20° for strongly water wet calcite system (personal communication), and contact angles greater than 20° would make the discrepancy between oil-water and mercury Pcs even worse. Very scarce results have been published on Hg_v-Hg_l-solid systems. Churaev [23], Smithwick [24] or Latorre et al. [25] presented contact angle data which were significantly different from the usual (θH_{gv}=40°, [1]). Their results might suggest that the mercury contact angle increases when the capillary radius decreases (Figure 8). This figure also shows the mercury contact angle (vapour phase) which is necessary to reconcile the oil-water and mercury Pc curves as a function of throat pore size (derived from MICP and Laplace Eq.). The mercury contact angle ranges from θH_{gv}=40° to 60° for all microporous facies with a significant trend of increasing mercury contact angle as the throat size decreases. In figure 8, the results obtained on the R4 facies are less clear. These results are interpreted by the accessibility to large pores by fine pore throats. Comparisons between bimodal pore throat radii histogram obtained from mercury injection (see figure 9) and large pore observed by X-Ray microtomography image acquired at ESRF (F) (see figure 10) support such an interpretation. It should be noted also that the discrepancy between water-oil and mercury Pcs was minimal in R4 compared to microporous facies. The influence of pore angularity (α) and contact angle has been checked using the MS-P models (Ma et al. [26]). Figure 5 shows that variation in pore geometries (cylindrical, α=1° or α=30°) do not explain such differences on Pc curves and do not support trends observed by Masalmeh [6] or Newsham [7]. Finally, pellicular films cannot offer a valid explanation for the initial difference in wetting phase saturation, as discrepancies appear even in very high water saturation range.

Influence of contact with reservoir oil or severe oil base mud invasion

Figure 11a shows the primary drainage Pc curves for different fluid couples (Ma-w, Li-w, La-w) for the R4 facies. Pc curves are very similar, whatever the oil type (crude or refined). Figure 11a also shows the Pc curves, for the same couples of fluids, but after ageing with crude oil, cleaning with organic solvents and a new primary drainage test [Aged_Cleaned]. This process is deemed representative of samples originating from oil-bearing reservoirs and used for primary drainage tests. Only minor discrepancies (less than 5 s.u.) are observed between the initial and the subsequent primary drainage Pcs. Finally, Figure 110a shows the primary drainage Pc curves of samples centrifuged with

oil base Mud after an initial primary drainage with refined oil, followed by cleaning [Mud_Cleaned]. Samples invaded by mud filtrate exhibit a very low water saturation (Swi=1%) at high Pc. After cleaning, a subsequent primary drainage leads to a very pessimistic water saturation at high Pc (Swi= 20%), compared to the Sw after the initial primary drainage with refined oil (Swi=7.7%).
Results obtained on Orgon samples are rather similar (see figure 11 b). Again, the types of oil used for primary drainage at initial strongly water wet conditions do not exert a significant influence on the results. But, after ageing and cleaning, Swi is always slightly larger compared to the initial primary drainage, whatever the crude oil characteristics (Li or La). Finally, Pc curves derived from core previously invaded by oil base mud and cleaned are pessimistic (Swi = 29%) compared to the initial drainage with refined oil before mud contamination (Swi = 7.5%). In conclusion, those results show that severe oil base mud invasion can dramatically bias the determination of primary drainage Pc even after cleaning and the bias will be case dependent.

Pore structure dependence of Wettability Index
Amott Harvey wettability indexes to water (I_{AHw}) for different treatments applied on facies R4, R3 and Orgon are gathered on Figure 7a. I_{AH} indexes obtained at the end of each full Amott Harvey cycle (see Table 2) are summarized on Figure 7b. Those observations clearly illustrate that: (1) using Ma52®-brine, all facies present strong water affinity, even if R4 samples are slightly less water wet than Orgon; (2) primary drainage in ambient temperature using crude oil (Li or La) only slightly affects wettability, the water wetness remains strong; (3) The ageing process shifts the water wetness towards lower values for R4 samples, has a limited effect on R3 and Orgon remains strongly water-wet. Water spontaneous imbibition curves rates (see Figure 12) confirm those results. It is generally thought that carbonates are oil-wet. This general statement is neither confirmed by our study nor by other recent results: Tie [28] showed that a limestone core from the Mt Gambier outcrop was still water-wet after being aged for ten days at 75°C with the Cottonwood or Minnelusa reservoir oils. As our observations are made for identical fluid systems and mineralogy (pure calcite), same equivalent maximum Pc and Swi, wettability variations might be attributed to the topological differences between facies. The visualization of R4 and Orgon porous media puts in evidence two important observations: 1) the microporous fractions show strong similarities between the two facies: see Figure 13 and pore throat radius derived from MICP (see Figure 9) 2) Orgon consists only of microporosity whereas half of the porous media can be ascribed to a macroporous fraction on R4 (see Figure 14). Skauge's [27] interpretation of the origin of mixed wet media, based on the stability of thin wetting films, could offer an explanation to the contrast between the two samples. Skauge suggests that, amongst concave pore configurations, the critical pressure needed to collapse water films is lower on large pores than in thin pores. Accordingly, the wettability of the R4 samples has also seen been significantly more altered than for Orgon. It might be due to an easier film collapse in the macroporous fraction of R4 which is absent in Orgon.

It was shown that oil base mud invasion can significantly bias the determination of primary drainage Pc curve. Figures 7 and 15 confirm that the strong initial wettability to water has been significantly altered in such a case.

Efficiency of cleaning process

After aging with crude oil at reservoir temperature and cleaning, initial wettability indexes are almost restored for Orgon and R3 but not for R4. It might indicate that the cleaning is less efficient in rocks exhibiting bimodal pore size distribution (R4) than unimodal pores distribution (R3 and Orgon) (see also figure 9). Wettability was altered on samples subjected to severe mud invasion but the spontaneous imbibition test after cleaning suggests that strongly water-wet conditions were restored after cleaning (see figure 15). This last result is paradoxical as, after severe oil base mud invasion and cleaning, the drainage Pc curves for refined oil are widely different from those achieved initially (fig. 10). Pore network modelling was used to decipher this contradiction. The model described in reference [29] was anchored on water-oil drainage Pc curves of the Orgon samples. Both porosity and permeability were very well reproduced. Simulation of the spontaneous imbibition at strongly water-wet conditions is in excellent agreement with experimental data: the amount of spontaneous imbibition is 38% and 41% respectively (see figures 15 and 16a). Another simulation of 1st drainage and 1st imbibition was carried out assuming that the contact angle before the 1st drainage varies from 0 to 97 degrees according to a truncated Weibull distribution. Figure 16b shows that the simulation captures three main features of the drainage and imbibition experimental data: 1) the plateau of the drainage Pc curve with weak, distributed water wetness is achieved at much weaker Pc than with strong, uniform water wetness. 2) the residual water saturation obtained with weak, distributed water wetness is much larger than with strong, uniform water wetness. 3) A significant water imbibition may still occur with weak, distributed water wetness.

However, the agreement between the experimental and simulated drainage Pc curves after flush with OBM and cleaning is far from perfect. The ability to assign the contact angles as a function of pore sizes prior to the 1st drainage might be required to better describe the experimental results but was not available.

CONCLUSIONS

- Large discrepancies are observed in the scaling of water/oil and mercury injection Pc curves, particularly in microporous facies. Discrepancies are very significant over the full saturation range. Suggestions related to the mercury contact angle and its possible variation with throat radius have been proposed.
- Severe oil base mud invasion may result in dramatic overestimate of the initial water saturation from 1st drainage Pc, even after core cleaning.
- Wettability variations within a carbonate reservoir might also be attributed to the topological differences between facies.

- The efficiency of cleaning processes in carbonates is dependent on the interplay between the macroporosity and the microporosity, for the same reservoir oil and for the same suite of solvents.
- "Irreducible" water saturation is a poor criterion for rock-typing in carbonates.

AKNOWLEDGMENTS

The authors would like to thank TOTAL Exploration Production for permission to publish this work. They also thank Pascal Clament (TOTAL) for his helpful contributions.

REFERENCES

[1] Purcell, W.R. Capillary pressures - Their measurement using mercury and the calculation of permeability there from. Pet. Trans. AIME., 1949, 186, 39-48.
[2] Melrose J.C., Dixon, J.R. Comparison of different techniques for obtaining capillary pressure data in the low-saturation region. SPE 22690, 66 th ATCE, Dallas, USA, October 1991.
[3] Sabatier, L. Comparative study of drainage capillary pressure measurements using different techniques and for different fluid systems. SCA-9424, 1994, p. 12.
[4] Hamon, G., Pellerin, F.M. Evidencing capillary pressure and relative permeability trends for reservoir simulation, SPE 38898, 1997, p. 12.
[5] Greder, H.N., Gallato, V., Cordelier, Ph, Laran, D., Munoz, V., d'Abrigeon, O. Forty comparisons of mercury injection data with oil/water capillary pressure measurements by the porous plate technique. 1997, SCA-9710, p.13.
[6] Masalmeh, S.K., Jing, X.D. Carbonate SCAL: Characterization of carbonate rock types for determination of saturation functions for determination of saturation functions and residual oil saturations. 2004, SCA2004-08, p. 12.
[7] Newsham, K.E., Rushing, J.A., Lasswell, P.M., Blasingame, T.A. A comparative study of laboratory techniques for measuring capillary pressures in tight gas sands. 2004, SPE 89866, p. 11.
[8] Wells, J.D., Amaefule, J.O. Capillary pressure and permeability relationships in tight gas sands, SPE 13879, SPE Low Permeability Gas reservoirs: Denver, USA, May 1985.
[9] Morrow, N.R. Capillary pressure correlations for uniformly wetted porous media. 1976, Journal of Canadian Petroleum Technology, Preprint n° 7619, p. 49-69.
[10] Morrow, N.R., McCaffery, F.G. Fluid Displacement Studies in Uniformly Wetted Porous Media. 1978, Wetting, Spreading and Adhesion, Ed. J.F. Padday, Academic Press, New York, p. 289-319.
[11] Richardson J.G., Holstein E.D. Comparison of water saturation from capillary pressure measurements with oil-base mud cores data, Ivishak (Sadlerochit) reservoir, Prudhoe Bay field. SPE 28593, 69th ATCE, New Orleans, USA, September 1994.
[12] Treiber, L.E., Archer, D.L., Owens, W.W. A laboratory evaluation of the wettability of fifty oil-producing reservoirs. 1972, SPE 3526, p.531-540.
[13] Anderson, W.G. Wettability literature survey-Part 6: The effect of wettability on waterflooding. 1986, Journal of Petroleum Technology, p. 1605-1622.

[14] Dunham,R.J. Classification of carbonate rocks according to depositional texture. 1965, In: Classification of carbonates rocks, Ham, W.E. (ed.), p. 108-121.
[15] Forbes, P. Quantitative evaluation and correction of gravity effects on centrifuge capillary pressure curves. 1997, SCA-9734, p. 14.
[16] Anderson, W.G. Wettability litterature survey - Part 2: Wettability measurments. 1986, Journal of Petroleum Technology, p. 1246-1262.
[17] Cuiec, L. Wettability laboratory evaluation under reservoir conditions: A new apparatus. 1995, SCA-9529, p. 12.
[18] Cuiec, L., Bieber, M.T., Jacquin, C., Conrard, P., Labastie, A., Morineau, Y., Nectoux, A. Détermination de la mouillabilité d'un échantillon de roche-réservoir. 1978, Revue de l'Institut Françcais du Pétrole, vol. 23, n°5, p. 705-728.
[19] Xie, X., Morrow, N.R. Oil recovery by spontaneous imbibition from weakly water-wet rocks. 2001, Petrophysics, vol.42, n°4, p. 331-322.
[20] Zhou, X., Morrow, N.R., Ma, S. Interrelationship of wettability, initial water saturation, aging time and oil recovery by spontaneous imbibition and waterflooding. 2000 SPE 62507, vol. 5, n°2, p. 199-207.
[21] Zhang, X., Morrow, N.R., Ma, S. Experimental verification of a modified scaling group for spontaneous imbibition. 1996, SPE 30762, p. 280-285.
[22] Forbes, P. Centrifuge data analysis techniques: A survey from the SCA. On the calculation of capillary pressure curves from centrifuge measurements. 1997, SCA, p.183.
[23] Churaev, N.V., Sobolev, V.D., Somov, A.N. Slippage of liquids over lyophobic solid surfaces. 1983, Journal of Colloid and Interface Science, vol.97, n°2, p.574-581.
[24] Smithwick III, R.W. Contact-angle studies of microscopic mercury droplets on glass. 1987, Journal of Colloid and Interface Science, vol.123, n°2, p. 482-485.
[25] Latorre,L., KIM, C.J., Leeuwen, J.V., Guzman,P.P., Nouet P. Electrostatic actuation of microscale liquid metal droplets: analysis, experiment, and FEM simulation. 2002, Journal of Microelectromechanical Systems, vol. 11, n° 4, p. 302-308.
[26] Ma, S., Mason, G., Morrow, N.R. Effect of contact angle on drainage and imbibition in regular polygonal tubes. 1996, Colloidal and Surfaces A: Physicochemical and Engineering aspects, n°117, p. 273-291.
[27] Skauge, A., Spildo, K., Hoiland, L., Vik, Ottesen B. Experimental evidence of different intermediate wetting states. 2004, SCA 2004-04, p. 12.
[28] Tie, H., Tong, Z., Morrow, N.R.: " The effect of Different Crude-oil/Brine/rock combinations on wettability through spontaneous imbibition" 2003, SCA 2003-02, p14-15
[29] Valvatne, P.H, Blunt, M.J.: "Predictive pore-scale modelling of two-phase flow in mixed-wet media" Water Resources Research, vol. 40, W07406, July 2004

TABLES

Oil	Density (22°C, g.cm^{-3})	μ_o (22°C,cp)	$\sigma_{oil\text{-}water}$ (22°C, dynes.cm^{-1})
Li (Crude Oil)	0.865	14.4	21.6
La (Crude Oil)	0.855	7.3	19.2
Ma (Refined Oil)	0.837	11.5	40-45
Oil base mud filtrat	0.809	4.1	5.7

	Density (22°C,g.cm^{-3})	[NaCl] (kg.m^{-3})	[KCl] (kg.m^{-3})	[$MgCl_2.6H_2O$] (kg.m^{-3})	[$CaCl_2.6H_2O$] (kg.m^{-3})
Brine	1.028	33.3	4.25	1.77	5.72

Table 1: Selected properties of crude oil, refined oil and oil base mud filtrate (left) synthetic brine composition (right).

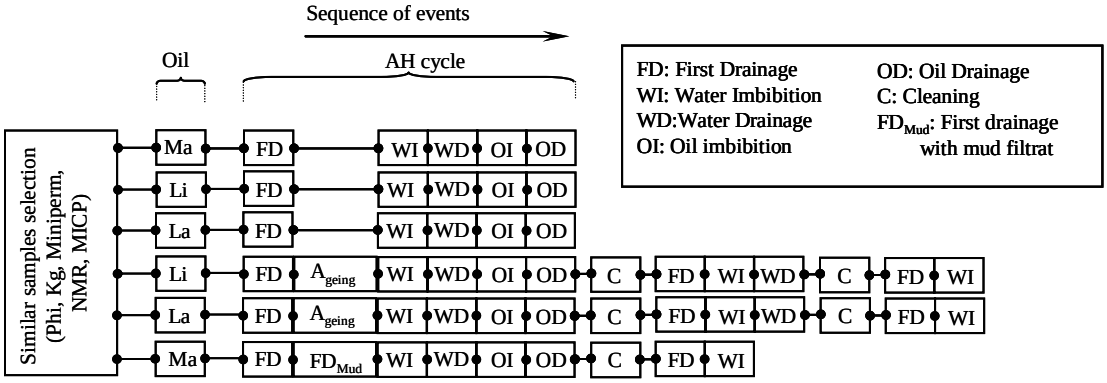

Table. 2: Experimental procedures. This flow-chart was applied for the 3 main sedimentary facies, R3, R4 and Orgon.

FIGURES

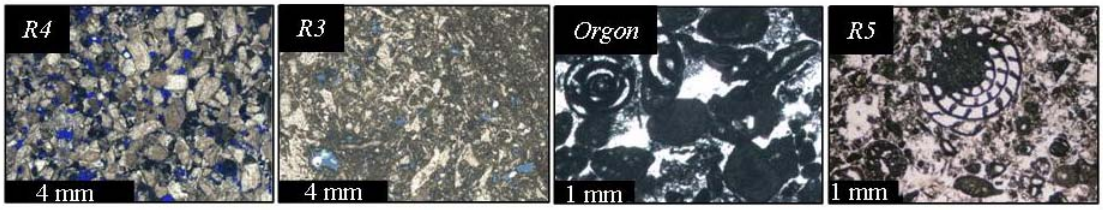

Figure 1: Thin section images of the 4 sedimentary facies which have been used in the present study; R4 and R3 facies present macroporous fraction (in blue) which is missing in Orgon or R5 (full microporous facies).

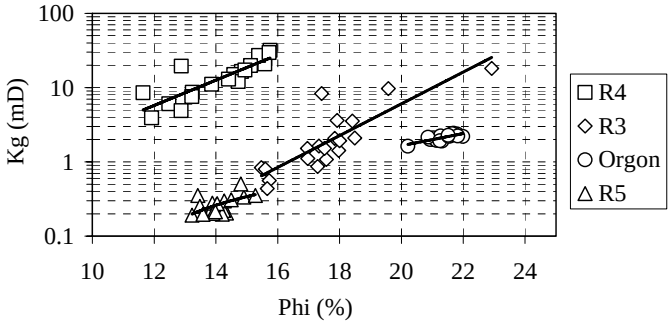

Figure 2: Porosity (Phi) and gas permeability (Kg).

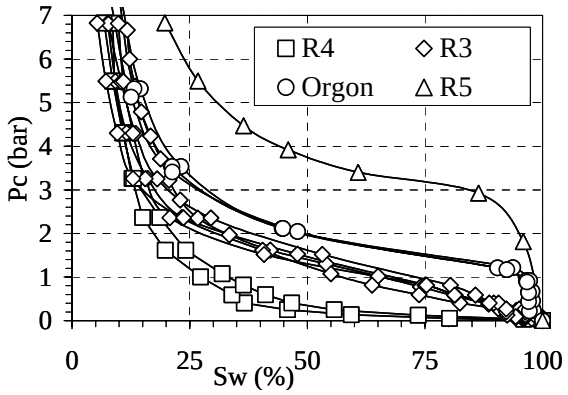

Figure 3: Comparing centrifuge Pc Curves porosity (MA_{52}®/brine @ 40 dynes.cm^{-1}) from each sedimentary facies.

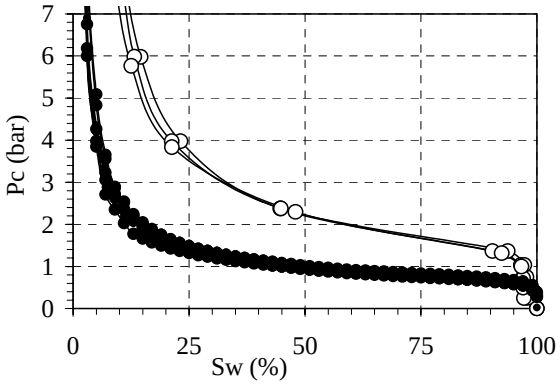

Figure 4: Comparing centrifuge (MA_{52}®/brine @ 40 dynes.cm^{-1}, white circles) system to Hg-Air Pc curves on facies Orgon (Hg_{vap}-Hg_{liq} converted @ 40 dynes.cm^{-1}, black circles); θHg_v=0°, θ_{w-o}=0°.

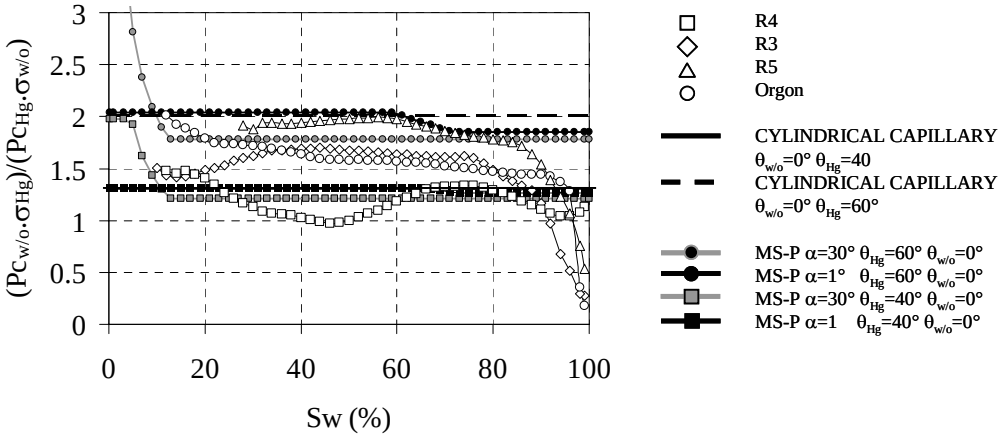

Figure 5: Comparing experimental Pc ratio (centrifuge to Hg-Air) for our 4 sedimentary facies and geometrical model MS-P (Ma et al., 1996) using different angularity (α) and contact angle (θ).

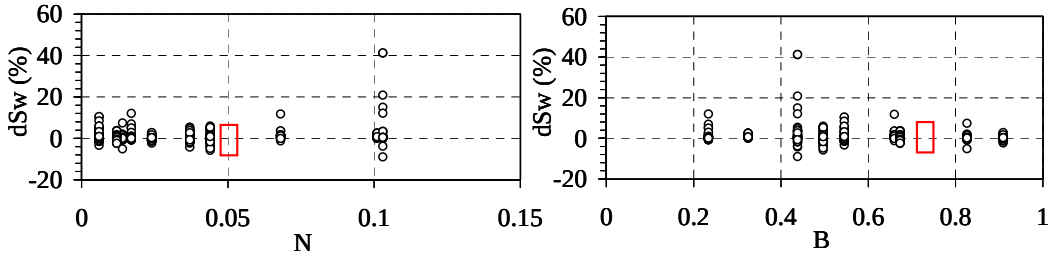

Figure 6: Error of saturation related to B and N values obtained in SCA survey (Forbes, 1997) for the Forbes interpretation method of Pc curves. The squares point out our range of values for B and N in our study.

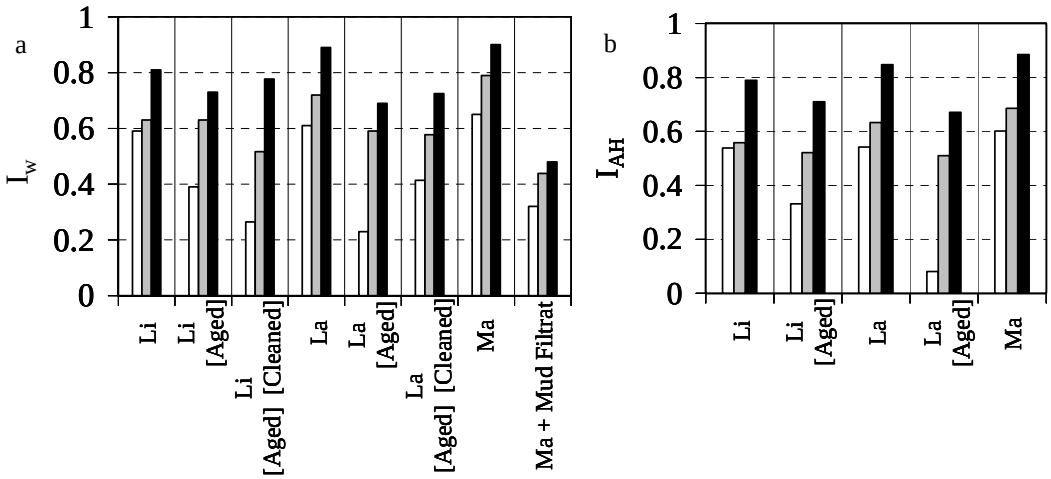

Figure 7: a) Influence on Water wettability Index of crude oil (Li, La), refined oil (Ma), mud filtrate invasion (Ma+Mud) and experimental procedures ([Aged], [Aged] [Cleaned]) on R4 (white), R3 (grey), Orgon (black); b) Influence on Amott Harvey wettability Index of crude oil (Li, La), refined oil (Ma) mud filtrate invasion (Ma+Mud) and aging procedure ([Aged]) on R4 (white), R3 (grey), Orgon (black).

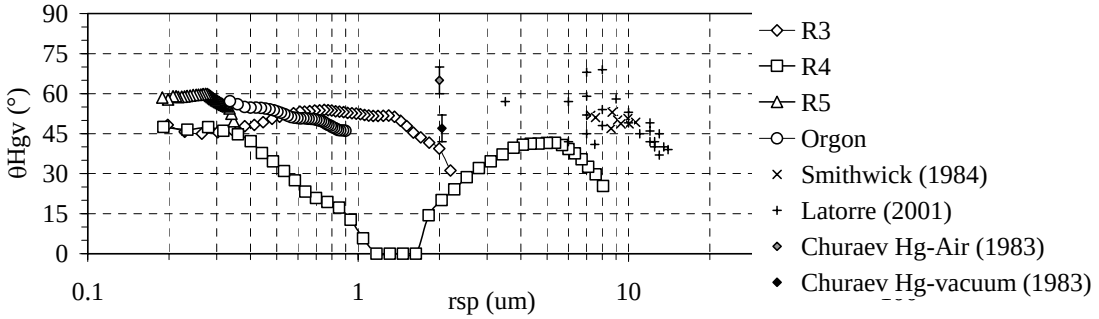

Figure 8: Mercury contact angle (air phase) necessary to reconcile the water oil and Hg Pc curves as a function of throat pore size.

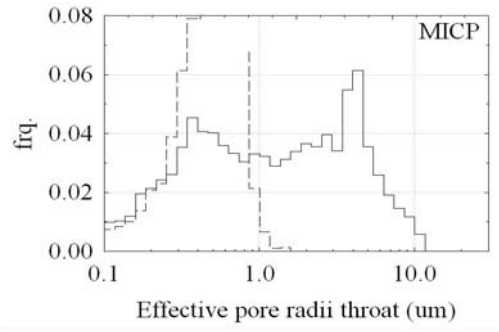

Figure 9: Pore throat radii for the bimodal R4 (blacks lines) and unimodal Orgon (dashed lines) porous media.

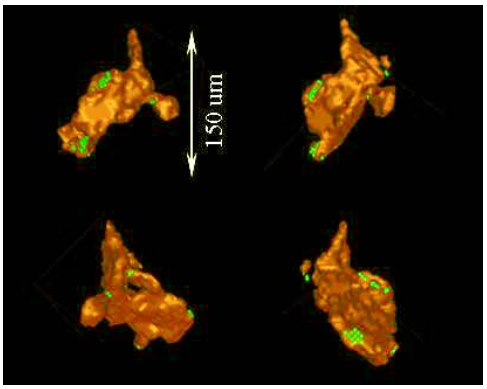

Figure 10: X-Ray Microtomographic images of a pore from R4 macroporous fraction. Connections with adjacent pores are represented by green voxels.

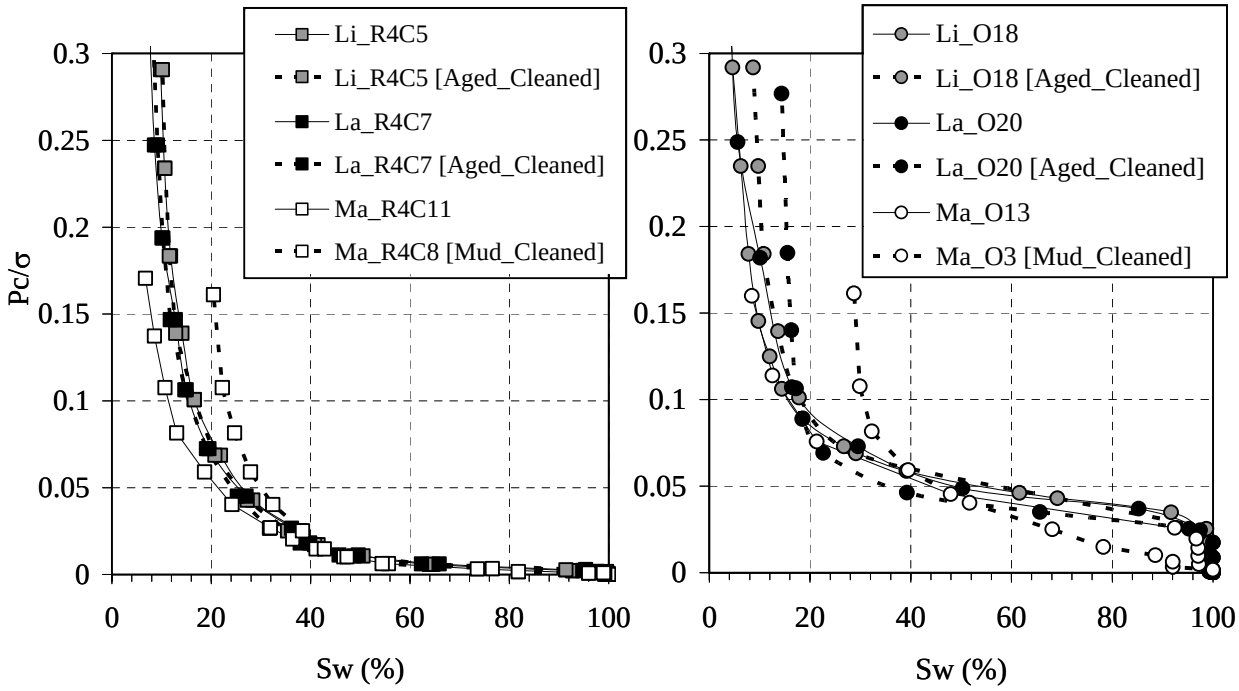

Figure 11: Influence of refined oil (Ma), crude oil (Li and La), Ageing followed by a cleaning [Aged_Cleaned], Mud filtrate followed by a cleaning [Mud_Cleaned] on first drainage capillary pressure curves for facies R4 (left) and Orgon (right). Text in brackets corresponds to experimental procedures applied in previous cycle for a same sample.

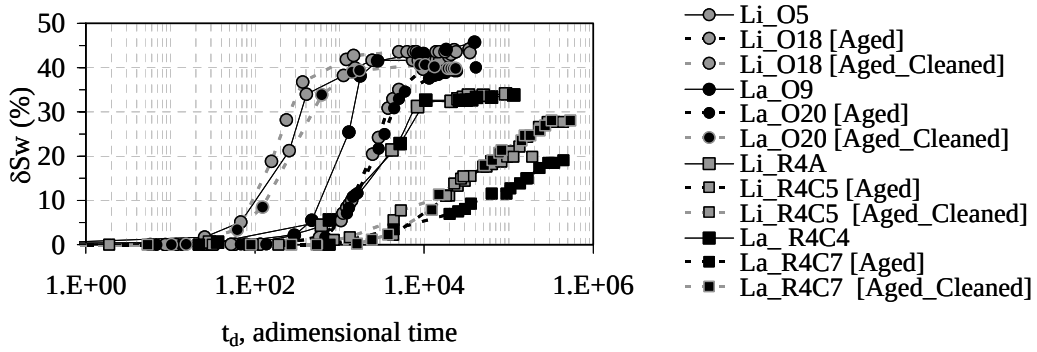

Figure 12: Influence of crude oil (Li, La), Ageing ([Aged]), and Cleaning ([Aged_Cleaned]) on water spontaneous imbibition For Orgon and R4 facies.

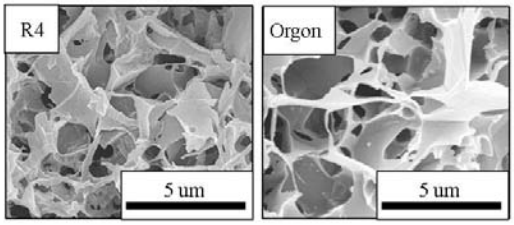

Figure 13: Porecasts of R4 and Orgon microporosity (SEM Images).

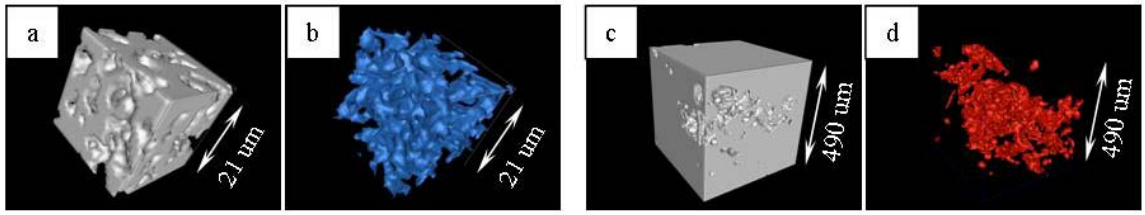

Figure 14: X-Ray Microtomographic images; a and c: Solid phases of Orgon (microporous fraction) and R4 (macroporous fraction): b, d: pore surfaces of Orgon (microporous fraction) and R4 (macroporous fraction).

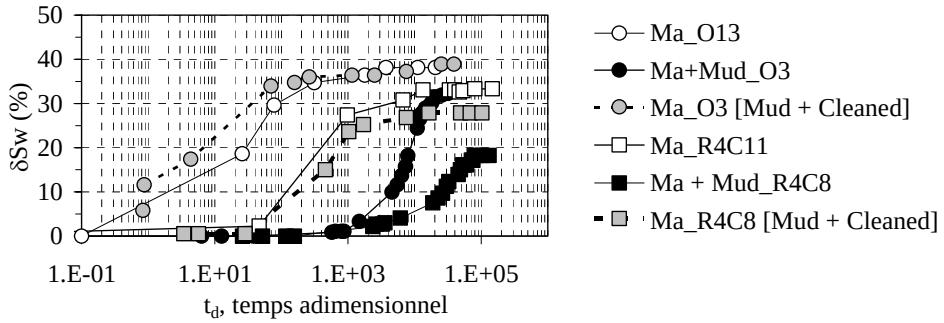

Figure 15: Influence of Mud invasion (Ma+Mud), followed by cleaning ([Mud + Cleaned]) on water spontaneous imbibition.

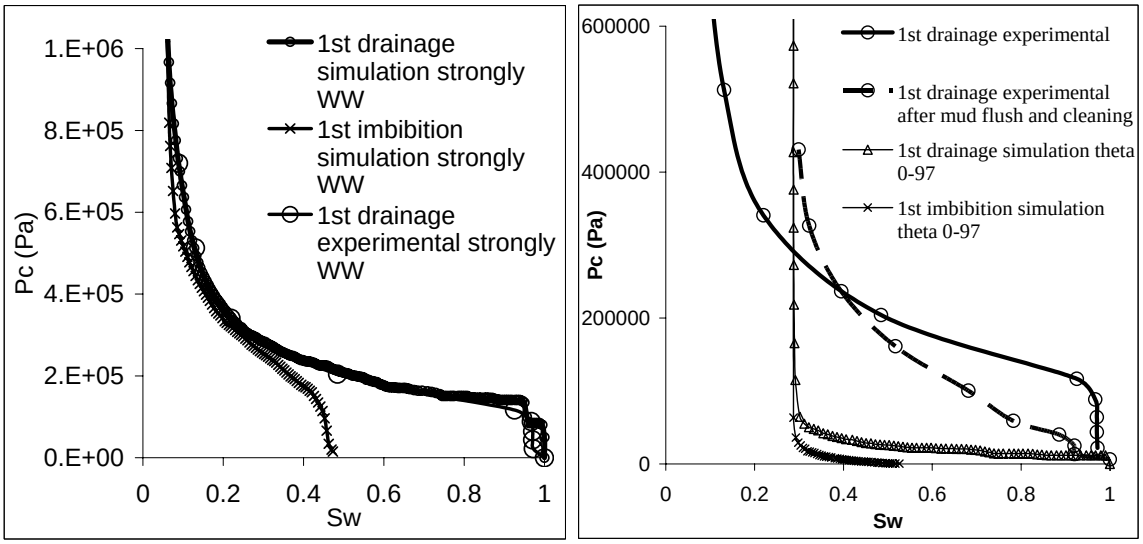

Figure 16 : simulation of 1st drainage and imbibition with uniform (0 deg; left)and truncated weibull (0-97 deg; right) distribution of contact angles and comparison with experimental results.